The Microfabrication of Capacitive Ultrasonic Transducers

X. C. Jin, I. Ladabaum, and B. T. Khuri-Yakub
E. L. Ginzton Laboratory, Stanford University, Stanford, CA 94305

Abstract— **The successful fabrication of surface micromachined ultrasonic transducers is reported. In a key step of the microfabrication, amorphous silicon is used as a sacrificial layer to form sealed nitride cavities. The process is fully CMOS compatible and allows for improved geometric control compared to previously reported work. Transmission experiments in both water and air are presented. A dynamic range in excess of 110dB is observed in air at 2.3MHz. In water, a single pair of transducers is able to operate from 2MHz to 20MHz. When tuned, a 3MHz tone burst results in a received signal with better than 60dB signal to noise ratio. The transducer behavior agrees with theoretical understanding of transducer dynamics.**

Keywords— **Micromachining, Ultrasonic Transducer, Capacitive Transducer**

I. Introduction

Ultrasound is used in a wide variety of applications which can be characterized as either sensing modalities or actuating modalities. Examples of sensing applications include medical imaging, non-destructive evaluation (NDE), ranging, and gas flow metering. As an actuating mechanism, ultrasound is used in industrial cleaning, soldering, and medical therapy. For years, piezoelectric ceramics and engineering cleverness have enabled a significant number of ultrasonic devices and systems [1]. But fruitful applications are restricted by the piezoelectrics' limitations. Piezoelectric transducers require strict geometric tolerances, which in turn limit possible array configurations and electrical characteristics. Furthermore, piezoelectrics depole at relatively low temperatures. As an alternative, capacitive ultrasonic transducers are some of the most promising candidates.

Micromachined ultrasonic transducers (MUTs) are an advanced configuration of capacitive transducers. In recent years, progress has been reported in theoretical understanding [2], [3], [4], [5], [6], [7] and implementations [8], [9], [10], [11], [12], [13] of MUTs.

In contrast to previous publications, this paper focuses on the realization of designs based on the reported theoretical understanding, and more specifically, the microfabrication process. Computer simulations are used to obtain geometric parameters, and lithographic and thin film techniques enable the realization of such geometries.

II. Fabrication

A MUT consists of metalized membranes (top electrode) suspended above heavily doped silicon bulk (bottom electrode). A schematic of one element of the device is shown in Fig. 1. A transducer consists of many such elements. When a DC voltage is applied between the two electrodes, coulomb forces attract them together. At the same time, the residual stress within the membrane resists the attraction. If the membrane is driven by an AC voltage, significant ultrasound generation results. Conversely, significant detection currents are generated when the membrane is biased appropriately and subjected to ultrasonic waves.

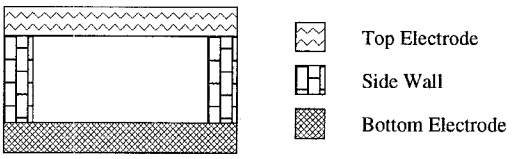

Fig. 1. *Schematic of one element of a MUT.*

The fabrication scheme of the MUTs used to generate the results herein reported is found in Fig. 2. It is fully compatible with standard CMOS fabrication processes.

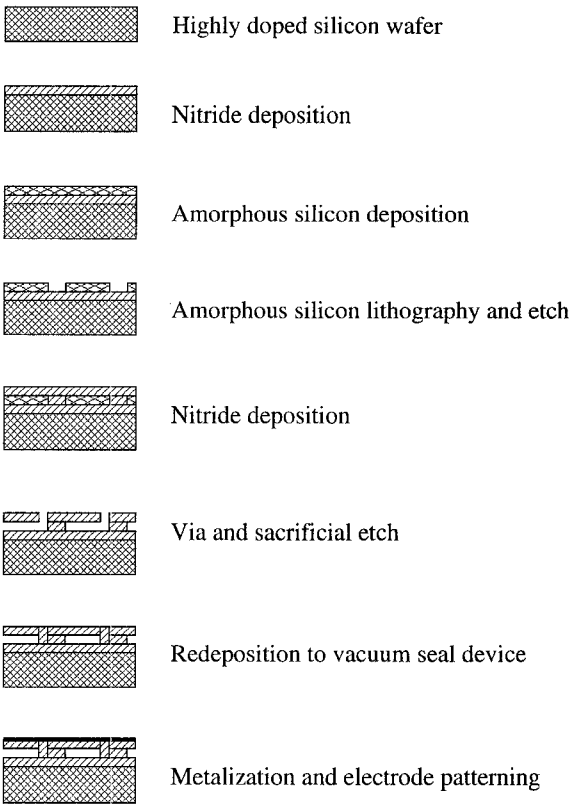

Fig. 2. *Major steps of MUT fabrication.*

A 4 inch n-type (100) silicon wafer is heavily doped with phosphorus gas phase drive-in to achieve good conductivity at the wafer surface. A thin layer of LPCVD nitride is then deposited at 800°C as an etch stop in the KOH sacrificial etching to be performed later. Amorphous silicon is subsequently deposited at 560°C to form the sacrificial layer. The thickness is typically around 2000Å to 1um depending

on whether the transducer will be used in gases, or liquids, as a receiver, or a transmitter. Deposited amorphous silicon is patterned into hexagonally shaped islands to define the active transducer regions. The maximum dimension of the hexagon ranges from 30um in immersion operation to 100um in air operation. The mechanical resonance frequency is a strong function of this dimension.

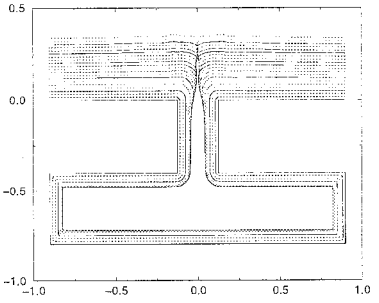

Fig. 3. *SPEEDIE simulation for sealing from top.*

A second layer of nitride is then deposited by LPCVD at 800°C to form a thin membrane. The silane and ammonia ratio is controlled such that desired residual stress is obtained. Both the residual stress and membrane thickness affect the resonant frequency and the voltage at which an electrostatic pull-in phenomenon is observed. Vias are dry-etched to allow sacrificial etching in KOH at 75°C. The dimension of the via has implications on the mechanism with which subsequent vacuum sealing is performed. SPEEDIE simulation [14] indicates that it is easier to seal from the top with a lower sticking coefficient species when the via has submicron dimensions. Fig. 3 is a computer simulated result of a successfully sealed cavity with a quarter micron via by LPCVD nitride deposition at 800°C. This sealing mechanism was verified in previous work [12]. When the via opening is a few microns wide, it is more convenient to seal from the bottom with a higher sticking coefficient species. Fig. 4 is a SPEEDIE simulation result verifying a sealed cavity with a 2um via by LTO deposition at 400°C. An SEM of such LTO sealing is found in Fig. 5.

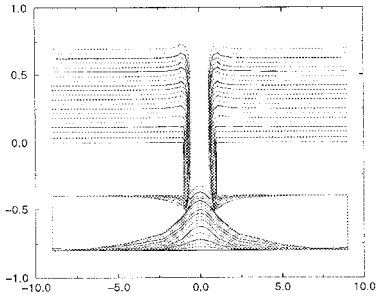

Fig. 4. *SPEEDIE simulation for sealing from bottom.*

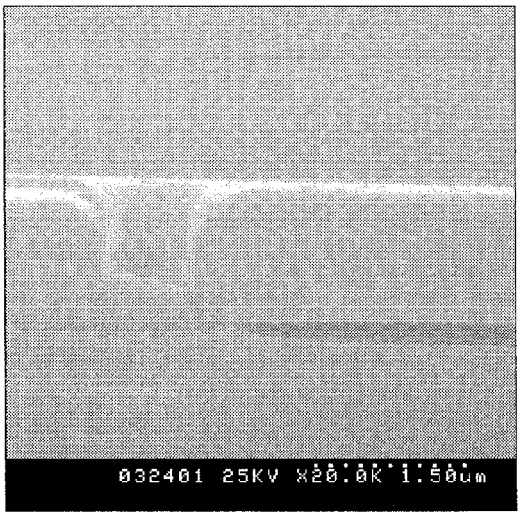

Fig. 5. *SEM of LTO sealing.*

Finally, aluminum is sputtered and patterned to act as the top electrode. The same aluminum deposition also defines bonding contacts to the bottom electrode through a lithographically defined trench in silicon bulk. An SEM of the top view of the transducer is shown in Fig. 6.

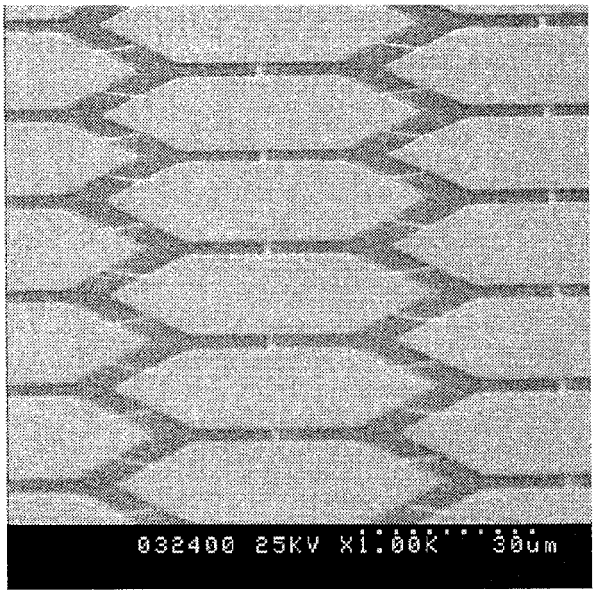

Fig. 6. *SEM top view of the MUT.*

III. Results

The experiments in this paper are performed with the help of a simple in-house electronic set-up. Time domain data are captured with an 8-bit digitized oscilloscope and frequency domain data are captured with a network analyzer. Subsequently the data are transferred to a computer for display. In certain circumstances, data sample averaging is performed to obtain better signal to noise ratio (SNR). The AC excitation signal is provided by a pulse

function generator with 50Ω output resistance. A custom transconductance amplifier conditions the received signal.

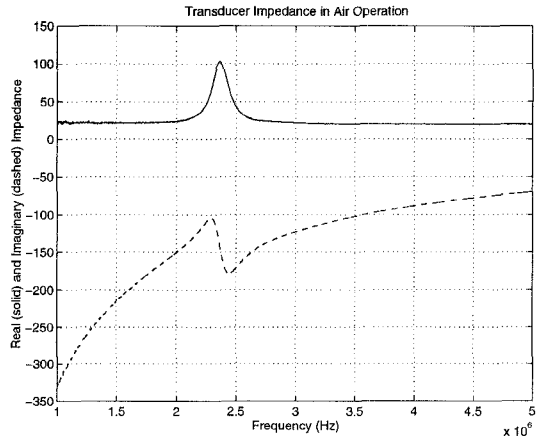

Fig. 7. *Transducer impedance with air loading.*

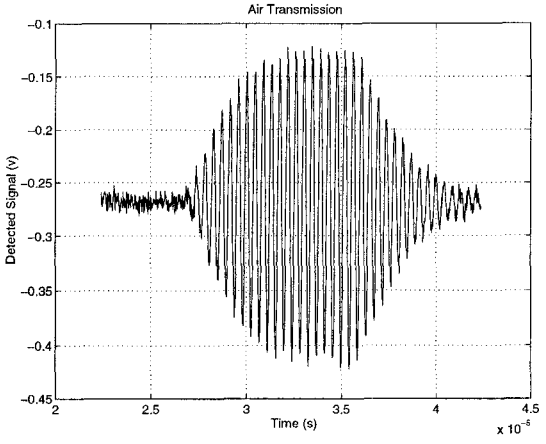

Fig. 8. *20 cycle burst transmission in air at 2.3MHz.*

Fig. 7 shows the impedance of an air transducer with a resonant frequency at 2.3MHz. It has comparable real and imaginary impedance at resonance. This makes it possible to tune out the imaginary part with a serial inductor without severely degrading bandwidth. As shown in Fig. 8, the receiver is able to detect the ultrasound transmitted in air with better than 30dB SNR after 16 sample averages. This result is obtained when a 20 cycle, 10mv tone burst is applied to the transmitter at a 2.3MHZ resonant frequency. Here, both transmitter and receiver transducers are $1cm^2$ and are biased with 30v DC voltage. When AC excitation is increased to 10v, and the transducers are more carefully tuned, a dynamic range in excess of 110dB is observed in air operation after 64 sample averages [7].

In fact, the same device can be used for both air and water transmission since the fabrication process is designed to yield vacuum sealed cavities. But a good air transducer is not necessarily the best immersion transducer due to the different loading effects of air and water. Fig. 9 shows the impedance of a transducer used in immersion operation. The real part of the transducer impedance is significantly lower than the real air-loaded impedance. When the receiver impedance is tuned with a serial inductor, better than 60dB SNR is observed in water transmission at 3MHz, as shown in Fig. 10. In the figure, electromagnetic feedthrough is followed by the acoustic signal indicating a 5mm physical separation. In this experiment, the receiver MUT is $0.25cm^2$ and the transmitter MUT is $1cm^2$. The lower dynamic range compared to air operation is mainly due to the higher imaginary-to-real impedance ratio. This leads to an impedance mismatch with transmitting and receiving electronics since the same electronic system is used for both air and water operation.

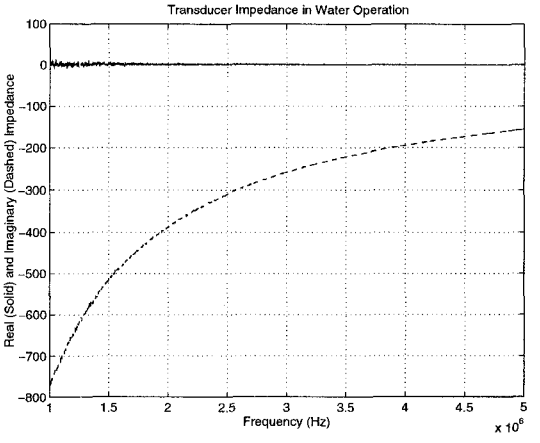

Fig. 9. *Transducer impedance with water loading.*

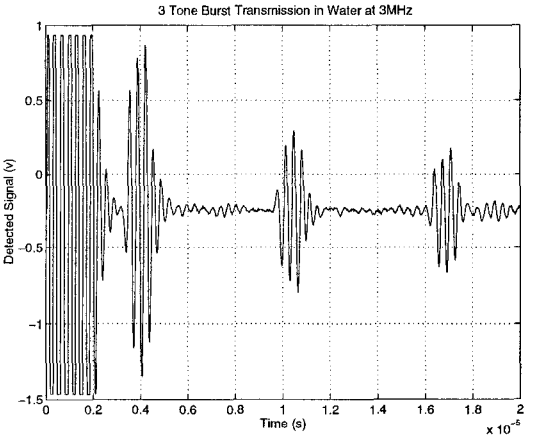

Fig. 10. *3 cycle burst transmission in water at 3MHz.*

Wide band transmission is possible if the MUTs operate less efficiently, which is true for untuned and unoptimized immersion transducers. Fig. 11 shows a single cycle transmission at 10MHz without data averaging. In this experiment, both the receiver and the transmitter are $1cm^2$. In future designs of immersion transducers, the geometry of the device (gap thickness, membrane thickness, and radius) and bias voltage of the device can be modified to optimize the transducers for water operation, or more specifically, to increase the absolute value of the real part of the transducer impedance to the level comparable to the electronics.

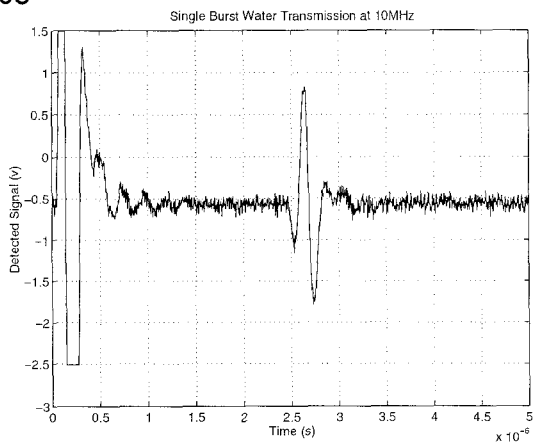

Fig. 11. *Single cycle water transmission at 10MHz.*

IV. Conclusion

This paper presents a fabrication scheme based on theoretical understanding of transducer dynamics, which results in working ultrasonic transducers. Amorphous silicon is used as a sacrificial layer to form sealed nitride cavities. It is important to appreciate the etching selectivity of silicon vs. nitride in KOH, which allows the realization of the design. A dynamic range in excess of 110dB is achieved in air at 2.3MHz. In water operation, a single pair of MUTs can transmit 2Mhz to 20MHz ultrasound. When tuned, a 3MHz tone burst results in better than 60dB SNR. It is anticipated that future optimized designs will result in better immersion operation.

The experiments show MUTs are a feasible alternative to piezoelectric transducers in many applications. Furthermore, MUTs can operate at much higher temperature (they do not have a Curie temperature), arrays can be fabricated at lower cost, and the electrical impedance of a MUT element can be designed to optimize the noise performance of receiver electronics.

V. Acknowledgement

This work has been made possible by grants from the United States Office of Naval Research. The first author would also want to acknowledge Fellowship support from the National University of Singapore.

References

[1] G. S. Kino, *Acoustic Waves: Devices, Imaging, and Analog Signal Processing*, Prentice-Hall, Inc., 1987.

[2] M. I. Haller, *Micromachined Ultrasonic Devices and Materials*, Ph.D. thesis, Stanford University, 1996.

[3] Schindel, D. W., Hutchins, D. A., Zou, L., and Sayer, M., "The design and characterization of micromachined air-coupled capacitance transducers," *IEEE Transactions on Ultrasonics, Ferroelectrics, and Frequency Control*, vol. 42, no. 1, pp. 42–50, January 1995.

[4] Pentti, M., Tsuzuki, F., Vaataja, H., and Sasaki, K., "Electroacoustic model for electrostatic ultrasonic transducers with v-grooved backplates," *IEEE Transactions on Ultrasonics, Ferroelectrics, and Frequency Control*, vol. 42, no. 1, pp. 1–7, January 1995.

[5] Haller, M. I. and Khuri-Yakub, B. T., "A surface micromachined electrostatic ultrasonic air transducer," *IEEE Transactions on Ultrasonics, Ferroelectrics, and Frequency Control*, vol. 43, no. 1, pp. 1–6, January 1996.

[6] Ladabaum, I., Jin, X. C., Soh, H. T., Pierre, F., Atalar, A., and Khuri-Yakub, B. T., "Micromachined ultrasonic transducers: towards robust models and immersion devices," in *Ultrasonics Symposium*, San Antonio, USA, 1996, IEEE Ultrasonics, Ferroelectrics, and Frequency Control Society.

[7] Ladabaum, I., Jin, X. C., Soh, H. T., Atalar, A., and Khuri-Yakub, B. T., "Surface micromachined capacitive ultrasonic transducers," *IEEE Transactions on Ultrasonics, Ferroelectrics, and Frequency Control*, (submitted), 1997.

[8] Haller, M. I.and Khuri-Yakub, B. T., "A surface micromachined electrostatic ultrasonic air transducer," in *Ultrasonics Symposium*, Cannes, France, 1994, IEEE Ultrasonics, Ferroelectrics, and Frequency Control Society, pp. 1241–1244.

[9] Ladabaum, I., Khuri-Yakub, B. T., Spoliansky, D., and Haller, M. I., "Micromachined ultrasonic transducers MUTs," in *Ultrasonics Symposium*, Levy, M., Schneider, S. C., and McAvoy, B. R., Eds., Seattle, Washington, November 1995, IEEE Ultrasonics, Ferroelectrics, and Frequency Control Society, pp. 501–504.

[10] Schindel, D. W. and Hutchins, D. A., "Applications of micromachined capacitance transducers in air-coupled ultrasonics and nondestructive evaluation," *IEEE Transactions on Ultrasonics, Ferroelectrics, and Frequency Control*, vol. 42, no. 1, pp. 51–58, January 1995.

[11] Ladabaum, I., Khuri-Yakub, B. T., and Spoliansky, D., "Micromachined ultrasonic transducers: 11.4 mhz transmission in air and more," *Applied Physics Letters*, vol. 68, no. 1, pp. 7–9, January 1996.

[12] Soh, H. T., Ladabaum, I., Atalar, A., Quate, C. F., and Khuri-Yakub, B. T., "Silicon micromachined ultrasonic immersion transducers," *Applied Physics Letters*, vol. 69, no. 24, pp. 3674–3676, 1996.

[13] Eccardt, P., Niederer, K., Scheiter, T., and Hierold, C., "Surface micromachined ultrasound transducers in cmos technology," in *Ultrasonics Symposium*, San Antonio, USA, 1996, IEEE Ultrasonics, Ferroelectrics, and Frequency Control Society.

[14] McVittie, J. P., Bang, D. S., Han, J. S., Hsiau, K., Li, J., and Zheng, J., "Stanford profile emulator for etching and deposition in ic engineering," *SPEEDIE 3.0 Manual*, Center for Integrated Systems, Stanford University, 1995.